

Near Surface Phase Transition of SrTiO_3 Studied by Zero Field β -Detected Nuclear Spin Relaxation and Resonance

Z. Salman,¹ R.F. Kiefl,^{1, 2, 3} K.H. Chow,⁴ M.D. Hossain,² T.A. Keeler,² S.R. Kreitzman,¹ C.D.P. Levy,¹ R.I. Miller,¹ T.J. Parolin,⁵ M.R. Pearson,¹ H. Saadaoui,² J.D. Schultz,² M. Smadella,¹ D. Wang,² and W.A. MacFarlane⁵

¹TRIUMF, 4004 Wesbrook Mall, Vancouver, BC, Canada, V6T 2A3

²Department of Physics and Astronomy, University of British Columbia, Vancouver, BC, Canada V6T 1Z1

³Canadian Institute for Advanced Research, Canada

⁴Department of Physics, University of Alberta, Edmonton, AB, Canada T6G 2J1

⁵Chemistry Department, University of British Columbia, Vancouver, BC, Canada V6T 1Z1

The zero field nuclear quadrupole resonance (NQR) and spin relaxation of ${}^8\text{Li}$ was measured as a function of temperature near the surface of a SrTiO_3 single crystal. A dramatic loss of the ${}^8\text{Li}$ nuclear polarization is observed below the structural phase transition. We find that the transition near the surface occurs at $T_c \sim 150$ K, i.e. ~ 45 K higher than T_c^{bulk} . The NQR line has a temperature dependent resonance frequency and broadening, and disappears below T_c^{bulk} . We find no evidence for preferred orientation of the tetragonal domains formed below T_c .

Strontium Titanate (SrTiO_3) is a fascinating insulator exhibiting remarkable properties, such as “quantum paraelectricity” which can be relieved by oxygen isotope substitution[1]. It is also of significant practical importance as a substrate and buffer layer in electronic heterostructures. At room temperature, bulk SrTiO_3 adopts the cubic perovskite structure, but undergoes an antiferrodisplacive soft-mode structural phase transition to a tetragonal phase at $T_c^{\text{bulk}} \approx 105$ K. Intensive research on this second order transition has driven many advances in the general theory of structural phase transitions but has not itself yielded to complete understanding [2]. In particular, neutron scattering found that, in the critical regime above T_c , in addition to the conventional soft-mode inelastic peak, there was a sharp very intense quasielastic peak, indicating the critical fluctuations had not one, but two associated energy scales. Similarly, there were found two *lengthscales* for the critical fluctuations, with the longer arising from within $50 \mu\text{m}$ of the surface. This phenomenon has been further investigated to the micron length scale [3, 4]. From the opposite limit, the topmost atomic layers of SrTiO_3 have been probed by surface-sensitive techniques which find surface specific phenomena such as reconstruction [5].

In SrTiO_3 and more generally, changes to bulk phase transitions near a free surface are interesting both fundamentally and technologically. For example, it is predicted theoretically that T_c near the surface should be strongly enhanced [6]. Thus, it is important to bridge the gap between the top-atomic layer studies, and the “surface limit” of bulk techniques at the micron scale. There are relatively few probes of this depth range, but recently optical second harmonic generation (SHG) has been used in this context in SrTiO_3 [7]. Nuclear Magnetic Resonance (NMR), and the related technique of Nuclear Quadrupole Resonance (NQR), where the nuclear electric quadrupolar (rather than Zeeman) interaction is used to split the magnetic sublevels, is not generally surface-sensitive, though notable exceptions exist [8]. However, using a radioactive detection scheme, based on the par-

ity violating property of β -decay, one can, by implanting a low energy beam of radioactive probe nuclei, study structural phenomena in thin films [9], near [10, 11] and at surfaces [12], using the closely related, but much more sensitive, techniques of β -NMR and β -NQR.

In this paper we present zero magnetic field ${}^8\text{Li}$ β -NQR [10] and spin relaxation measurements near the surface of an epitaxially polished $\langle 100 \rangle$ single crystal of SrTiO_3 (Applied Technology Enterprises). The ${}^8\text{Li}$ beam is produced at the isotope separator and accelerator (ISAC) at TRIUMF. It is then spin-polarized using a collinear optical pumping method, yielding nuclear polarization as high as 70% [9, 10]. Since the implanted beam energy (28 keV) is relatively low, the implanted ${}^8\text{Li}$ stops at an average depth of $\sim 1500 \text{ \AA}$ from the surface.

Recently we reported the first zero field (ZF) NQR of ${}^8\text{Li}$ in SrTiO_3 at room temperature [10]. There we confirmed that ${}^8\text{Li}^+$ occupies the face center (F) site in the SrTiO_3 cubic lattice, experiencing an almost axially symmetric electric field gradient (EFG), $\frac{\partial^2 V}{\partial x_i \partial x_j}$, with symmetry axis along a cubic axis of the crystal [10, 11]. Since the ${}^8\text{Li}$ nucleus has spin $I = 2$ and an electric quadrupole moment $Q = +33 \text{ mb}$, the ZF spin Hamiltonian for ${}^8\text{Li}$ at the F site in SrTiO_3 can be written as

$$\mathcal{H}_q = \hbar \nu_q [I_z^2 - 2] \quad (1)$$

where $\nu_q = e^2 q Q / 8$ and $eq = V_{zz}$ is the EFG along the symmetry axis. The energy eigenvalues $E_m = \hbar \nu_q (m^2 - 2)$ are a function of the azimuthal quantum number m where $I_z |m\rangle = m |m\rangle$. Hence, in ZF there are two possible resonance frequencies at ν_q and $3\nu_q$ corresponding to the allowed magnetic dipole transitions $0 \leftrightarrow \pm 1$ and $\pm 1 \leftrightarrow \pm 2$. In our experiments most of the ${}^8\text{Li}$ nuclei are prepared in either $|+2\rangle$ or $| -2\rangle$ spin states, and therefore we expect only the resonance at $3\nu_q$.

In this experiment, ${}^8\text{Li}$ ions are implanted with their nuclear polarization, $\mathbf{p}(0) = p_0 \hat{z}$, perpendicular to the $\langle 100 \rangle$ direction of the crystal. The time dependence of the ${}^8\text{Li}$ nuclear polarization along its initial direction, $p_z(t)$, can be measured through the β -decay asymmetry [9, 10].

${}^8\text{Li}$ occupies one of three equivalent F sites, where $\mathbf{p}(0)$ has three different orientations relative to the local EFG. In two sites, $\mathbf{p}(0)$ is perpendicular to the EFG's principal axis, and in the third it is parallel. The contribution of the first two sites to $p_z(t)$ rapidly averages to zero, since $\mathbf{p}(0)$ precesses at frequency $3\nu_q$, much higher than the experimental time resolution. Thus, the observed $p_z(t)$ is only that of the third site. Indeed we find that the initial polarization, $p_z(0)$, in ZF is about 1/3 of the full polarization measured in a high external magnetic field, $B \gg (\nu_q/\gamma)$ ($\gamma = 630.15 \text{ Hz/G}$ is the gyromagnetic ratio of ${}^8\text{Li}$).

Changes in the lattice or the symmetry of the ${}^8\text{Li}$ site will alter the EFG experienced by the ${}^8\text{Li}$ nucleus. A change in the strength of the EFG will cause a shift of the resonance frequency, while a deviation from axial symmetry of the ${}^8\text{Li}$ site will introduce non-axial components embodied in an additional term in the Hamiltonian,

$$H_\eta = \eta \nu_q (I_x^2 - I_y^2), \quad (2)$$

where $\eta = (V_{xx} - V_{yy})/V_{zz}$ is the conventional dimensionless EFG asymmetry parameter [13, 14]. This term introduces mixing between the $|\pm 2\rangle$ spin states with a characteristic frequency splitting $\Delta_{\pm 2} \simeq 3\eta^2\nu_q$ [10], and therefore a loss of polarization on the timescale $1/\Delta_{\pm 2}$. In general, for a structural phase transition, the size and/or symmetry of the EFG tensor may change, affecting the resonance as well as the polarization $p_z(t)$.

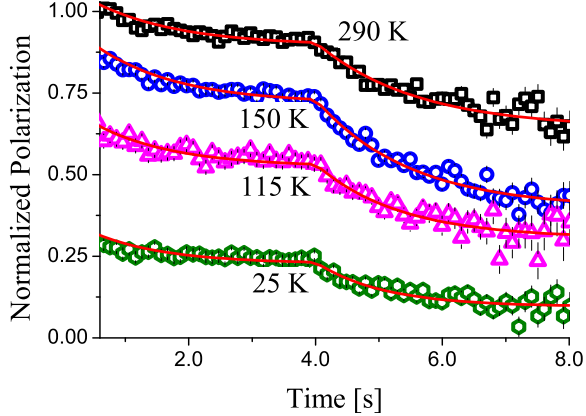


FIG. 1: The polarization as a function of time, normalized to its initial value at $T = 290 \text{ K}$, at several temperatures.

In the measurements reported here, the SrTiO_3 sample was mounted on a coldfinger cryostat in an ultra high vacuum (UHV) environment. Thermal contact between the sample and coldfinger was achieved with a small amount of UHV compatible grease (Apiezon N). The temperature gradient between the sample and diffuser of the cryostat was measured to be less than 0.2 K.

The polarization of ${}^8\text{Li}$ as a function of time, $p_z(t)$, is measured by implanting a pulse of ${}^8\text{Li}$ at a rate of about $10^6/\text{s}$, starting at $t = 0$ for a period of $\Delta = 4$ seconds, and measuring the β -decay asymmetry both during and

after the beam period. Measurements of $p_z(t)$ at different temperatures are shown in Fig. 1. The initial polarization was normalized to its value at room temperature.

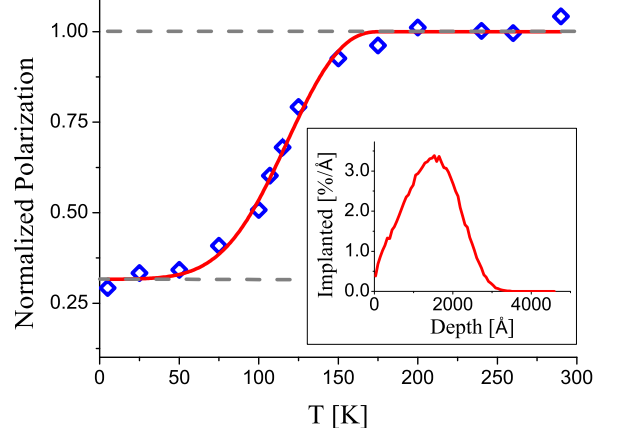


FIG. 2: The normalized initial polarization as a function of temperature. The solid line is a guide to the eye. The inset is the calculated ${}^8\text{Li}$ stopping profile.

The time evolution of the polarization, $p_z(t)$, is determined by both the ${}^8\text{Li}$ spin-lattice relaxation rate λ and its radioactive lifetime $\tau = 1.21\text{s}$. For a short pulse occurring at t_p and a general spin relaxation function $f(t, t_p : \lambda)$, the polarization follows

$$p_z(t) = \begin{cases} \frac{\int_0^t e^{-(t-t_p)/\tau} f(t, t_p : \lambda) dt_p}{\int_0^t e^{-t/\tau} dt} & t \leq \Delta \\ \frac{\int_0^\Delta e^{-(\Delta-t_p)/\tau} f(t, t_p : \lambda) dt_p}{\int_0^\Delta e^{-t/\tau} dt} & t > \Delta. \end{cases} \quad (3)$$

The data in Fig. 1 are fit to Eq. 3 with a phenomenological biexponential form,

$$f(t, t_p : \lambda) = A_1 e^{-\lambda_1(t-t_p)} + A_2 e^{-\lambda_2(t-t_p)}. \quad (4)$$

The relaxation rates from the fits are small (in particular one is ≈ 0) and do not vary much with temperature. In contrast, the amplitude $p_z(0) \equiv A_1 + A_2$, exhibits a strong temperature dependence (see Fig. 2). At high temperature $p_z(0) = 1$ independent of temperature, but decreases dramatically below 150 K, reaching $\sim 1/3$ below 75 K, where it becomes temperature independent. We attribute this loss of polarization to nonaxial components of the EFG which arise as the crystal's symmetry is lowered at the phase transition.

The tetragonal distortion below T_c , where c becomes larger than a , introduces non-axial distortion in the EFG for 2/3 of the ${}^8\text{Li}$ sites. We now must distinguish between two sites where c is perpendicular to the EFG's principal axis (F_{\perp}), and the third (F_{\parallel}) where it is parallel (see inset of Fig. 3). Treating the lattice of SrTiO_3 as an array of point charges, we calculated η for both types of F sites as a function of temperature, using the bulk lattice constants reported in Ref. [15]. As can be seen in Fig. 3,

η is exactly zero for all three sites in the cubic phase. It remains unchanged through the phase transition for the F_{\parallel} site, while for the two F_{\perp} sites, it increases up to $\sim 0.35\%$. This is due to the tetragonal distortion, which breaks the axial symmetry of the EFG at the two F_{\perp} sites, but not at F_{\parallel} . Note that in Ref. [10] we concluded that even at room temperature in the cubic phase, η is small but non-vanishing, which may be a consequence of symmetry-lowering due to random strain fields or possibly to a slight off-centre site for ${}^8\text{Li}$. The increase in η at T_c causes an increase in $\Delta_{\pm 2}$ sufficient to produce a loss of the polarization due to ${}^8\text{Li}$ at the F_{\perp} site. Our

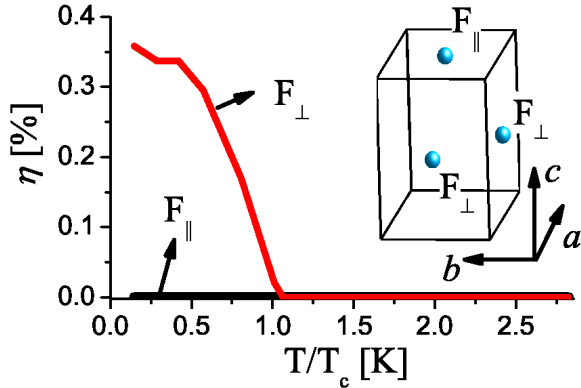


FIG. 3: The calculated η as a function of temperature. The inset shows the different types of ${}^8\text{Li}$ sites in SrTiO_3 unit cell.

experimental observation that the polarization is non-zero in the tetragonal phase indicates that a fraction of the implanted ${}^8\text{Li}$ still experiences an axially symmetric ($\eta \simeq 0$) EFG along its polarization, corresponding to ${}^8\text{Li}$ in the F_{\parallel} site. The $1/3$ value is further evidence that the c -axis of the tetragonal domains is oriented randomly, in agreement with Ref. [16].

The loss of polarization starts at $T_c \simeq 150$ K, much higher than the T_c^{bulk} . We attribute this enhancement of T_c to proximity to the nearby free surface of the crystal. Based on an extrapolation of the penetration depth dependence of the x-ray scattering parameters, an increase of $\Delta T_c = 220$ K was predicted [17]. SHG studies recently found that the phase transition near the surface of SrTiO_3 occurs $\Delta T_c = 45$ K above the temperature of the bulk phase transition [7]. A similar result was found closer to the surface by electron diffraction [18]. Unlike these techniques, the ${}^8\text{Li}$ nuclei sense the phase transition at the atomic scale, while the net signal is averaged over ${}^8\text{Li}$ sites in the implantation volume, which is a beamspot about 3 mm in diameter together with an implantation depth profile. The stopping of ion beams in matter is well-understood, and several reliable Monte Carlo codes are available to accurately calculate implantation profiles. We used the TRIM.SP package [19] to calculate the stopping distribution of 28 keV ${}^8\text{Li}^+$ in SrTiO_3 . The resulting depth profile (inset of Fig. 2) has an average implantation depth of ~ 1500 Å, a width (range straggling) of ~ 2000 Å, and a maximum depth

of ~ 3000 Å. Thus the spectra are composed of signals from ${}^8\text{Li}$ stopping at varying distances from the surface. The lower symmetry at the surface (together with effects such as surface reconstruction [5]) certainly presents a perturbative influence on the bulk structural phase transition. A simple model of this effect is to assume that T_c is a monotonically decreasing function of depth, falling from a maximal value at the surface (T_c^{surf}) to T_c^{bulk} at large depths. In this picture, the observed breadth of the

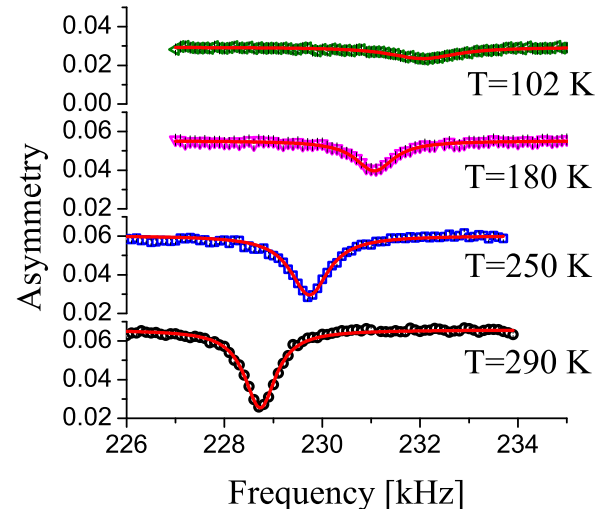


FIG. 4: ${}^8\text{Li}$ β -NQR lines in SrTiO_3 for different temperatures. The line shifts, broadens and weakens as the sample is cooled from room temperature to 100 K. The solid lines are fits to a Lorentzian.

transition is due, at least in part, to averaging over the intrinsically inhomogeneous T_c distribution (weighted by the implantation profile). The remarkable similarity of our estimate of T_c^{surf} to that of the surface-related reflection SHG signal [7], suggests a common intrinsic origin to the enhancement of T_c .

The β -NQR resonance was also measured from room temperature down to ~ 75 K, below which it could not be observed. The immediate loss of $2/3$ of the polarization for ${}^8\text{Li}$ stopping in tetragonal domains (where the phase transition has occurred) implies that the main contribution to the resonance comes from ${}^8\text{Li}$ stopping in the cubic phase. Therefore we expect the resonances to be less sensitive to the structural phase transition near the surface, since at 150 K they will be dominated by ${}^8\text{Li}$ stopping far from the surface. The resonance lines for several temperatures are presented in Fig. 4. Most noticeable is the large shift in the resonance frequency, reflecting an increase in the EFG. The ${}^8\text{Li}$ β -NQR lines fit very well to a single Lorentzian. The resonance frequency from the fits, $3\nu_q$, as a function of temperature is shown in Fig. 5. The value of $3\nu_q$ increases down to ~ 100 K, where it appears to saturate.

The temperature dependence of $3\nu_q$ is consistent with an increase of the EFG at the ${}^8\text{Li}$ site, due to thermal contraction of the SrTiO_3 lattice. In a point charge model,

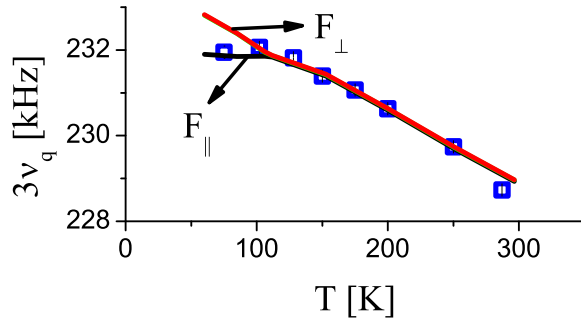


FIG. 5: The resonance frequency, $3\nu_q$, as a function of temperature, obtained from fitting the lines to a Lorentzian shape. The solid lines are the calculated value of $3\nu_q$.

the value of the EFG is simply proportional to $1/a^3$, where a is the lattice constant. While the absolute values of ν_q from a point charge calculation are not expected to agree well with measurements [13], the relative increase in $3\nu_q$ as a function of temperature (solid lines in Fig. 5) using the lattice constants reported in Ref. [15] yields very good agreement with the experiment from 290 K down to 105 K. The bifurcation of the calculated values at $T = 105$ K is due to the phase transition. At this temperature ν_q for the F_{\parallel} site becomes temperature independent, while it continues to increase for the F_{\perp} sites. The experimental results at low temperature agree with the calculated results for the F_{\parallel} site only, and there is no

evidence for a signal from the two F_{\perp} sites, confirming our previous conclusion that below the transition, η for these sites becomes large (see Fig. 3) and consequently their polarization is lost, and they do not contribute to the resonance.

In conclusion, we find that the structural phase transition temperature near the surface in SrTiO_3 is $T_c \sim 150$ K. We believe this increase is related to the surface. There was no evidence for a preferred direction of the c -axis of the tetragonal domains formed below the transition, i.e. their c -direction is oriented along any axis with equal probability. Although the cubic symmetry of SrTiO_3 is broken below the transition temperature, one of the ${}^8\text{Li}$ sites maintains a nearly axially symmetric EFG. Analogous studies to those reported here, but at different implantation energies (and therefore stopping depths) will allow depth-profiling of the surface proximity effect. We are currently augmenting our β -NQR spectrometer with a high voltage platform [9], in order to enable such a depth-resolved study. These results demonstrate, for the first time, that β -NQR can be used as a sensitive method for studies of structural phase transitions near the surface.

This work was supported by the CIAR, NSERC and TRIUMF. We thank Rahim Abasalti, Bassam Hitti and Donald Arseneau for technical support. We also thank Laura Greene for providing the SrTiO_3 crystal, W. Eckstein for providing the TRIM.SP code, and K.-C. Chou and W.J.L. Buyers for helpful discussions.

[1] e.g. see the review J. Dec, W. Kleemann, K. Boldyreva and M. Itoh *Ferroelectrics* **314**, 7 (2005).

[2] R.A. Cowley. *Phil. Trans. R. Soc. London A* **354**, 2799 (1996).

[3] R. Wang, Y. Zhu and S.M. Shapiro. *Phys. Rev. Lett.* **80**, 2370 (1998).

[4] H. Hünnefeld, T. Niemöller, J.R. Schneider, U. Rütt, S. Rodewald, J. Fleig and G. Shirane. *Phys. Rev. B* **66**, 014113 (2002).

[5] N. Erdman, K.R. Poeppelmeier, M. Asta, O. Warschkow, D.E. Ellis and L.D. Marks. *Nature* **419**, 55 (2002); J. Zegenhagen, T. Haage and Q.D. Jiang, *Appl. Phys. A* **67**, 711 (1998); K. Johnston, M.R. Castell, A.T. Paxton and M.W. Finnis. *Phys. Rev. B* **70**, 085415 (2004); B. Stauble-Pumpin, B. Ilge, V.C. Matijasevic, P.M.L.O. Scholte, A.J. Steinfort and F. Tuinstra. *Surf. Sci.* **369**, 313 (1996); G. Koster, G. Rijnders, D.H.A. Blank, H. Rogalla. *Physica C* **339**, 215 (2000).

[6] Structural: K. Binder and P.C. Hohenberg. *Phys. Rev. B* **9**, 2194 (1974); and Magnetic: D.L. Mills. *Phys. Rev. B* **3** 3887 (1971).

[7] E.D. Mishina, T.V. Misuryaev, N.E. Sherstyuk, V.V. Lemanov, A.I. Morozov, A.S. Sigov and Th. Rasing. *Phys. Rev. Lett.* **85**, 3664 (2000).

[8] e.g. P.K. Wang, J.P. Ansermet, S.L. Rudaz, Z. Wang, S. Shore, C.P. Slichter and J.H. Sinfelt, *Science* **234**, 35 (1986).

[9] G.D. Morris, W.A. MacFarlane, K.H. Chow, Z. Salman, D.J. Arseneau, S. Davel, A. Hatakeyama, S.R. Kreitzman, C.D.P. Levy, R. Poutissou, R.H. Heffner, J.E. Elejewski, L.H. Greene and R.F. Kiefl. *Phys. Rev. Lett.* **93**, 157601 (2004).

[10] Z. Salman, E.P. Reynard, W.A. MacFarlane, K.H. Chow, J. Chakhalian, S.R. Kreitzman, S. Davel, C.D.P. Levy, R. Poutissou and R.F. Kiefl. *Phys. Rev. B* **70**, 104404 (2004).

[11] W.A. MacFarlane, G.D. Morris, K.H. Chow, R.A. Baartman, S. Davel, S.R. Dunsiger, A. Hatakeyama, S.R. Kreitzman, C.D.P. Levy, R.I. Miller, K.M. Nichol, R. Poutissou, E. Dumont, L.H. Greene, and R.F. Kiefl. *Physica B* **326**, 209 (2003).

[12] e.g. H. Winnefeld, M. Czanta, G. Fahsold, H.J. Jänsch, G. Kirchner, W. Mannstadt, J.J. Paggel, R. Platzter, R. Schillinger, R. Veith, C. Weindel and D. Fick. *Phys. Rev. B* **65**, 195319 (2002); H.D. Ebinger, H.J. Jänsch, C. Polenz, B. Polivka, W. Preyss, V. Saier, R. Veith and D. Fick. *Phys. Rev. Lett.* **76**, 656 (1996).

[13] M.H. Cohen and F. Reif. *Solid State Physics* **5**, 321 (1957).

[14] T.P. Das and E.L. Hahn. *Nuclear Quadrupole Resonance Spectroscopy*. Academic Press Inc., 1958.

[15] A. Okazaki and M. Kawaminami. *Mat. Res. Bull.* **8**, 545 (1973).

[16] A. Buckley, J.P. Rivera and E.K.H. Salje. *J. Appl. Phys.* **86**, 1653 (1999).

[17] D.P. Osterman, K. Mohanty and J. Axe. *J. Phys. C* **21**,

2635 (1988).

[18] N.V. Krainyukova, M.A. Strzhemechny and A.P. Brodyanskii. *Czech. J. Phys.* **46**, 2685 (1996).

[19] W. Eckstein. *Computer Simulation of Ion-Solid Interactions*. Springer, Berlin, Heidelberg, New York, 1991.